Searching for signatures of dark matter-dark radiation interaction in observations of large-scale structure

Zhen Pan,[1,*] Manoj Kaplinghat,[2,†] and Lloyd Knox[1,‡]
[1]Department of Physics, University of California, Davis, California 95616, USA
[2]Department of Physics and Astronomy, University of California, Irvine, California 92697, USA

(Received 30 January 2018; published 29 May 2018)

In this paper, we conduct a search in the latest large-scale structure measurements for signatures of the dark matter-dark radiation interaction proposed by Buen-Abad *et al.* (2015). We show that prior claims of an inference of this interaction at $\sim 3\sigma$ significance rely on a use of the Sunyaev-Zeldovich cluster mass function that ignores uncertainty in the mass-observable relationship. Including this uncertainty we find that the inferred level of interaction remains consistent with the data, but so does zero interaction; i.e., there is no longer a preference for nonzero interaction. We also point out that inference of the shape and amplitude of the matter power spectrum from Lyα forest measurements is highly inconsistent with the predictions of the ΛCDM model conditioned on Planck cosmic microwave background temperature, polarization, and lensing power spectra, and that the dark matter-dark radiation model can restore that consistency. We also phenomenologically generalize the model of Buen-Abad *et al.* (2015) to allow for interaction rates with different scalings with temperature, and find that the original scaling is preferred by the data.

DOI: 10.1103/PhysRevD.97.103531

I. INTRODUCTION

Dark matter is an essential component of the standard ΛCDM cosmology, whose existence has been established from many cosmological and astrophysical lines of evidence (see e.g., [1–3] for a brief summary). On the other hand, increasingly sensitive efforts at direct detection of canonical candidates such as weakly interacting massive particles (WIMPs) and axions have only resulted in upper limits [4,5]. The lack of direct detection signatures implies that the dark matter is weakly coupled to the standard model, but it does not preclude a large coupling to a hidden sector. The idea of hidden sector dark matter has broadened the experimental search possibilities, while retaining some of the virtues of WIMP models such as concrete thermal and nonthermal production mechanisms (e.g., [6–9]) and opening up new cosmological signatures (e.g., [10,11]).

The richer phenomenology expands the possible ways in which dark matter properties may be revealed through observations of the large-scale structure (LSS) of the Universe. Precision measurement of the cosmic microwave background (CMB) temperature and polarization, as well as large-scale photometric and spectroscopic galaxy surveys can be used to detect the influence of nontrivial dark matter properties or to limit them [12]. Indeed, the σ_8 tension in ΛCDM cosmology, that LSS surveys yield lower σ_8 values than that derived from CMB observations, is potentially due to nontrivial dark matter interactions and has also served to renew interest in exploration of broader classes of dark matter models (e.g., [11,13–29]).

In this paper, we focus on the non-Abelian dark sector scenario proposed by [20], where the dark matter is a Dirac fermion that transforms under a non-Abelian gauge group, and the dark radiation is the associated gauge field, a massless "dark gluon." The strong self-interaction of the dark radiation makes it behave like a fluid, instead of a free-streaming species. The interaction between dark matter and the dark radiation fluid (dm-drf) acts to suppress the matter power spectrum, improving agreement with lower σ_8 values derived from LSS measurements [30–38]. Some previous works [21,26,28] show an inference of nonzero dm-drf interaction at 3σ significance jointly using Planck CMB and LSS measurements, including Planck CMB Lensing [30], CFHTLens weak lensing [31] and Planck Sunyaev-Zeldovich (SZ) cluster counters [37,38]. The authors of [21] also emphasize the possibility for these models to alleviate the H_0 tension [39,40] as well.[1]

Throughout this paper, we examine this non-Abelian dark sector model with these LSS measurements one by one. We critically review the analyses done previously and

*zhpan@ucdavis.edu
†mkapling@uci.edu
‡lknox@ucdavis.edu

[1]Recently, Das *et al.* [41] have proposed to use the history of cosmic reionization to constrain general dark matter-dark radiation interactions.

find that Planck SZ is essential for the claimed inference of nonzero dm-drf interaction in previous analyses. But the SZ cluster constraint is limited by a large uncertainty in the cluster mass scale determination, which is usually parametrized by a mass bias parameter b. The bias parameter b itself is constrained by several different analyses of the gravitational lensing induced by SZ galaxy clusters including two using the distorted shapes of background galaxies ("Weighing the Giants" [42] and the Canadian Cluster Comparison Project [43]) and one using distortions of the CMB [44]. The inferred value of σ_8 from the observations of the SZ clusters depends sensitively on the mass estimates of the clusters and therefore on the mass bias parameter b. While previous dm-drf analyses effectively assumed zero uncertainty in b, we find that including an uncertainty based on any of the above inferences of b, the claimed inference of nonzero dm-drf interaction turns into an upper limit.

We also consider constraints on the model from Lyman-α (Lyα) forest observations. This has been done previously by [26], using inferences of the matter power spectrum as reported in [45] in 2004. Here we use the more recent inference from the Baryon Oscillation Spectroscopic Survey Lyα forest observations [46–48]. Compared with the other LSS measurements mentioned above, the Lyα forest power spectrum is sensitive to the matter power spectrum at smaller scale $k \sim \mathrm{Mpc}^{-1}$, a scale that is more sensitive to the strength of the interaction in the dm-drf model. We find that the matter power spectrum derived from the latest Lyα forest data is much steeper than that derived from Planck CMB data, assuming ΛCDM. Finally, we examine whether this Lyα-CMB tension can be resolved by the dm-drf interaction, and whether the dm-drf interaction can lead to consistency across all the data sets we consider here.

The paper is organized as follows. In Sec. II, we briefly introduce the non-Abelian dark sector model and its impacts on the CMB power spectra and the matter power spectrum. Although these impacts have been calculated before, here we provide an explanation for the first time of why the impacts on the CMB power spectra are much smaller than on the matter power spectrum. In Sec. III, we show that using SZ data with the mass bias parameter fixed or varying makes a huge difference in the constraints of cosmological parameters. In Sec. IV, we point out the Lyα-CMB tension in the ΛCDM cosmology, and that the joint data set favors a nonzero dm-drf interaction. In Sec. V, we extend the exploration to more general dm-drf interaction models characterized by interaction rates scaling with temperature in different ways, and we also examine these models against CMB data and LSS measurements. We provide a summary in Sec. VI.

II. CANONICAL DM-DRF INTERACTION MODEL

Following Ref. [20], we use Γ for the momentum transfer rate [i.e., time scale for momentum of dark matter particles to change by $\mathcal{O}(1)$] due to the dm-drf scattering. This momentum transfer leads to a drag force on the nonrelativistic dark matter particles such that $\dot{\vec{v}}_{\rm dm} = a\Gamma(\vec{v}_{\rm drf} - \vec{v}_{\rm dm})$, where a is the scale factor and throughout this paper dots denote conformal time derivatives. In terms of physical quantities, Γ is approximately

$$\Gamma \simeq (T_{\rm drf}/m_{\rm dm}) n_{\rm drf} \sigma_{\rm dm-drf}, \tag{1}$$

where $m_{\rm dm}$ is the mass of dark matter particles, $\sigma_{\rm dm-drf}$ is the cross section of dm-drf scattering, and $T_{\rm drf}$ and $n_{\rm drf}$ are the temperature and the number density of dark radiation, respectively. For the non-Abelian dark sector model proposed by [20], $\sigma_{\rm dm-drf} \propto T_{\rm drf}^{-2}$; thus we can write $\Gamma = \Gamma_0 (T/T_0)^2$, where Γ_0 denotes the velocity change rate today. With this parametrization, the evolution equations of dark matter density and velocity perturbations, $\delta_{\rm dm}$ and $\theta_{\rm dm}$, and dark radiation density and velocity perturbations, $\delta_{\rm drf}$ and $\theta_{\rm drf}$, are written as [21]

$$\begin{aligned}
\dot{\delta}_{\rm dm} &= -\theta_{\rm dm} + 3\dot{\phi}, \\
\dot{\theta}_{\rm dm} &= \frac{\dot{a}}{a}\theta_{\rm dm} + k^2\psi + a\Gamma(\theta_{\rm drf} - \theta_{\rm dm}), \\
\dot{\delta}_{\rm drf} &= -\frac{4}{3}\theta_{\rm drf} + 4\dot{\phi}, \\
\dot{\theta}_{\rm drf} &= k^2\frac{\delta_{\rm dr}}{4} + k^2\psi + \frac{3\rho_{\rm dm}}{4\rho_{\rm drf}} a\Gamma(\theta_{\rm dm} - \theta_{\rm drf})
\end{aligned} \tag{2}$$

in the conformal Newtonian gauge, where $\rho_{\rm dm}$ and $\rho_{\rm drf}$ are the average densities of dark matter and dark radiation, respectively; ψ and ϕ are the Newtonian potential and the perturbation to the spatial curvature, respectively.[2]

In the remainder of this section, we qualitatively explain the impacts of dm-drf interaction on cosmological observables, by comparing the matter power spectra (Fig. 1) and CMB power spectra (Fig. 2) of three cosmologies with different parameters $\{N_\nu, N_{\rm drf}, \Gamma_0\}$ and same other parameters (see Table I). Similar numerical comparisons were also given in previous works [21,28], and here we focus on connecting the impacts on observables with underlying physics.

A. LSS

In the standard ΛCDM cosmology, the dark matter overdensity $\delta_{\rm dm}$ grows logarithmically in the radiation-dominated era, and grows linearly in the matter-dominated era (e.g., [50]). A small dm-drf interaction does not remove these growth modes; instead it decreases the corresponding growth rates. We define the overdensity suppression

[2]The perturbation evolution equations in the Boltzmann code CAMB are written in the synchronous gauge. In our modfied version CAMB, we keep a tiny amount of noninteracting dark matter to carry the synchronous gauge.

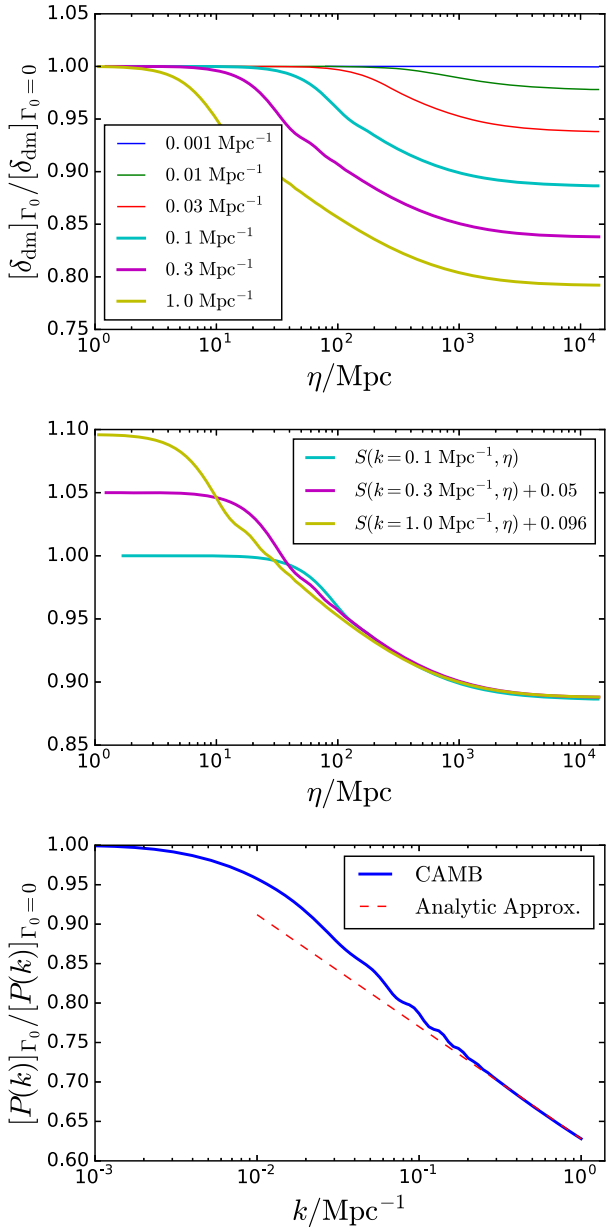

FIG. 1. Upper panel: the evolution of dark matter overdensity $\delta_{\rm dm}$ suppression for different k modes. Middle panel: the self-similar behavior of the overdensity suppression, where we displace the suppression of modes $k=0.3\ {\rm Mpc}^{-1}$ and $k=1.0\ {\rm Mpc}^{-1}$ by 0.05 and 0.096, respectively. Lower panel: the dm-drf interaction induced matter power spectrum suppression today, where the dashed line is an analytic fit in the form of Eq. (5).

function $\mathcal{S}(k,\eta)\equiv[\delta_{\rm dm}]_{\Gamma_0>0}/[\delta_{\rm dm}]_{\Gamma_0=0}$, and plot $\mathcal{S}(k,\eta)=[\delta_{\rm dm}]_{\rm Model\,3}/[\delta_{\rm dm}]_{\rm Model\,2}$ (Table I) for different k modes in Fig. 1. We see that $\mathcal{S}(k,\eta)$ shows a "self-similar" behavior for small-scale modes $k\gg k_{\rm eq}$: approximately,

$$\begin{aligned}&\mathcal{S}(k,\eta)=1 && (k\eta\lesssim 1),\\ &\mathcal{S}(k,\eta)\simeq 1-A\log(k\eta) && (1\lesssim k\eta\lesssim k\eta_{\rm eq}),\end{aligned}\tag{3}$$

and after radiation-matter equality, the evolution of $\mathcal{S}(k,\eta)$ is similar for all different modes, where the suppression at radiation-matter transition and that today differ by a constant number,

$$\mathcal{S}(k,\eta_{\rm eq})-\mathcal{S}(k,\eta_0)\simeq B,\tag{4}$$

where $1/k_{\rm eq}\approx\eta_{\rm eq}\approx 100$ Mpc, η_0 is the conformal time today, A and B are numbers independent of mode k and time η (for the example shown in Fig. 1, $A\approx 0.04$ and $B\approx 0.05$). The self-similar behavior for modes $k\gg k_{\rm eq}$ originates from the fact Γ/H is a constant in the radiation-dominated era, and therefore introduces no new time scale or length scale.

With the approximations above, we can estimate the power spectrum suppression today as

$$\begin{aligned}\frac{[P(k)]_{\Gamma_0>0}}{[P(k)]_{\Gamma_0=0}}&=(1-A\log(k/k_{\rm eq})-B)^2\\ &\approx 1-2B-2A\log(k/k_{\rm eq}),\end{aligned}\tag{5}$$

where we have ignored quadratic terms in the second line. This estimate explains the dm-drf interaction induced logarithmic suppression in the matter power spectrum $P(k)$ for modes $k\gg k_{\rm eq}$ (see Fig. 1 for the matter power suppression computed from CAMB and the logarithmic fit).

B. CMB

The imprint of the dm-drf interaction on the CMB power spectra is much more subtle as shown in Fig. 2. Comparison of models 1 and 2 confirms the signatures of free-streaming neutrinos in the CMB spectra: namely power suppression and a (very small) shift in acoustic peak locations [49–56]. Comparison of models 2 and 3 shows that the dm-drf interaction very slightly increases the amplitude of modes $\ell\lesssim 500$ and decreases that of modes $\ell\gtrsim 500$.

For modes $\ell\lesssim 500$, the increased amplitude can be explained by the near-resonant driving of the baryon-photon fluid perturbation amplitude by gravitational potential decay as modes enter the horizon [50–52]. The resistance to dark matter free fall from the dm-drf interaction contributes to gravitational potential decay, at least on scales large enough that, at the time of horizon crossing, the dark matter contributes a significant fraction of the total energy density.

For modes $\ell\gtrsim 500$, instead of an enhancement, we see instead a very small suppression of power and a small suppression of even-odd peak height difference due to the dm-drf interaction. The extra potential decay arising from the interaction changes the photon overdensity in two ways: amplitude suppression and baryon loading alleviation.

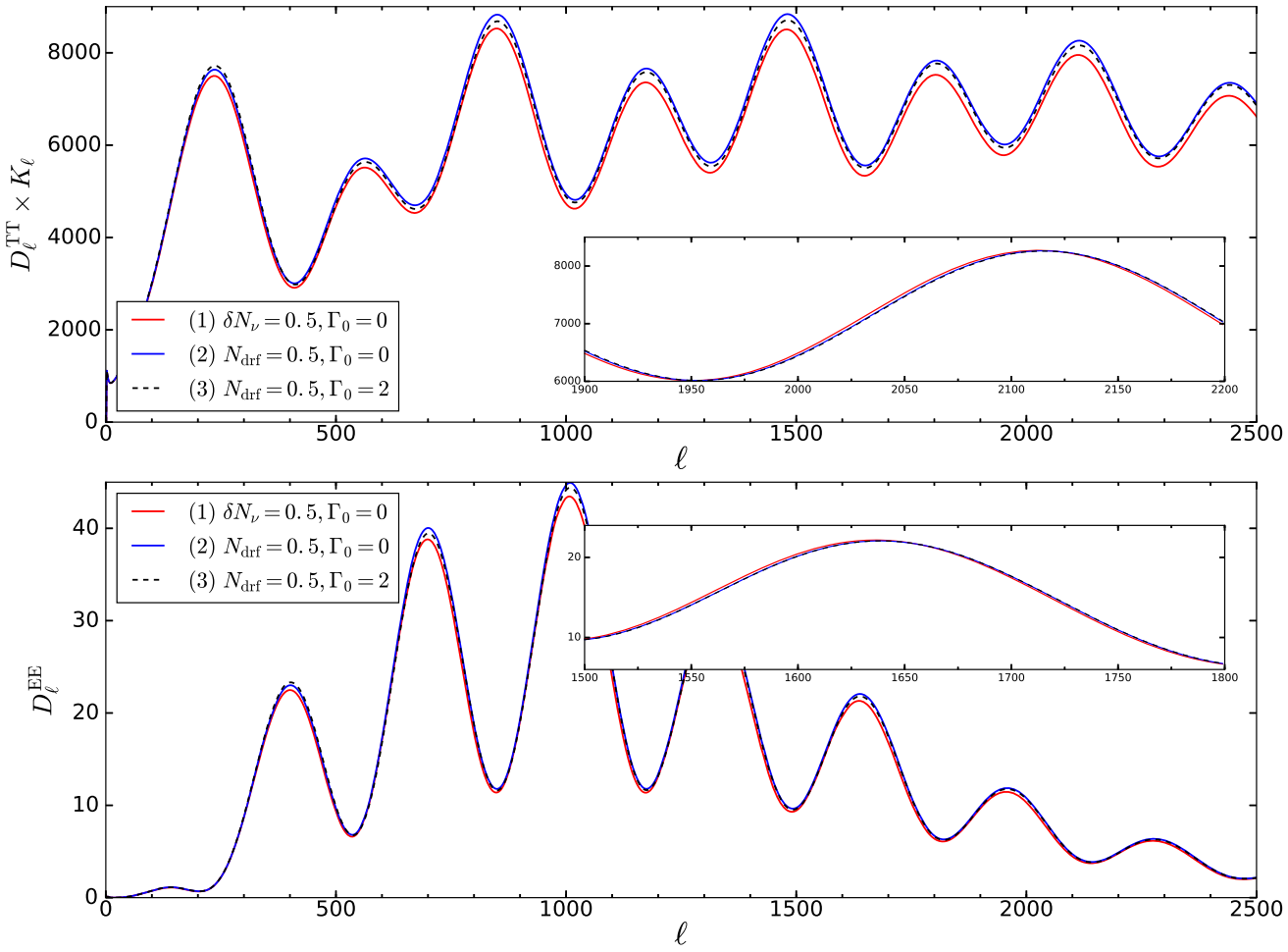

FIG. 2. Comparison of TT and EE spectra of the three models listed in Table I, where in the upper panel we plot the TT spectra with damping effect largely removed by multiplying a factor $K_\ell = \exp\{2 \times (\ell/1267)^{1.18}\}$; in the lower panel we plot the EE spectra, and in the two inset plots, we normalize the spectra amplitudes to allow one to see the impact of the very small shift in peak locations induced by free-streaming species as done in [49]. In these insets the red curve (the model with additional free-streaming neutrinos) is slightly shifted to the left relative to the dashed line and blue line which overlap each other.

At these small scales, we numerically find that the extra potential decay leads to a nearly uniform suppression of the photon perturbation amplitude in a low-baryon cosmology. We also find that the baryon loading effect is weaker in model 3 than in model 2. The two changes (amplitude suppression and baryon loading alleviation) add up constructively for the odd extrema ($kr_{s,*} = 3\pi, 5\pi, 7\pi$) and destructively for the even extrema ($kr_{s,*} = 2\pi, 4\pi, 6\pi$).[3]

TABLE I. Three models used for clarifying the impact of dark radiation fluid on cosmological observables, with different parameters $\{N_\nu, N_{\rm drf}, \Gamma_0\}$ and the same ΛCDM parameters $\omega_{\rm b} = 0.02253$, $\omega_{\rm dm} = 0.1122$, $A_{\rm s} = 2.42 \times 10^{-9}$, $n_{\rm s} = 0.967$, $\tau = 0.0845$, $H_0 = 70.4$ km/s/Mpc.

	N_ν	$N_{\rm drf}$	$10^7\Gamma_0({\rm Mpc}^{-1})$
Model 1	3.546	0.0	0
Model 2	3.046	0.5	0
Model 3	3.046	0.5	2

To summarize, the dm-drf interaction has a much smaller impact on the CMB power spectra than on the matter power spectrum. The impact on the matter power spectrum arises from interactions in the radiation-dominated era when the dark radiation has more inertia than the dark matter. The impact on the CMB power spectrum is through the impact on the dark matter evolution. On small scales, where the impact on dark matter is sizeable, the dark matter contribution to the gravitational potential at the time of horizon

[3]In fact, Planck CMB data are sensitive to the small suppression of the odd-even peak height difference. Our Markov chain Monte Carlo (MCMC) results show that the dm-drf model prefers a higher $\omega_{\rm b}$ than in the ΛCDM model.

crossing is very small and thus the net impact on the photon distribution is small.

III. PARAMETER CONSTRAINTS FROM LSS DATA

In this section, we first briefly review previous analyses of the implications of cosmological data for the extension of ΛCDM to include the dm-drf interaction model, identify Planck SZ as the major driver for the previously claimed inference of the nonzero dm-drf interaction, and redo the analysis with a treatment of uncertainties in the SZ-mass observable relationship.

A. Previous analyses

In previous analyses (e.g., [21,26,28]), Planck CMB and LSS measurements, including Planck CMB Lensing [30], CFHTLens [31] and Planck SZ [37,38],

$$\sigma_8(\Omega_m/0.27)^{0.25} = 0.820 \pm 0.029 \quad \text{[CMB Lensing]}, \tag{6a}$$

$$\sigma_8(\Omega_m/0.27)^{0.46} = 0.774 \pm 0.040 \quad \text{[CFHTLens]}, \tag{6b}$$

$$\sigma_8(\Omega_m/0.27)^{0.30} = 0.782 \pm 0.010 \quad \text{[Planck SZ]}, \tag{6c}$$

were used to constrain the dm-drf model, and the dm-drf interaction was detected at 3σ confidence level.

To figure out which data set is essential to the claimed inference of nonzero dm-drf interaction, we show the σ_8 tension of the ΛCDM cosmology in Fig. 3, which clearly shows that the SZ-CMB tension is the strongest. This finding also suggests that Planck SZ is driving the inference of nonzero dm-drf interaction.

The cosmological implications of the Planck SZ cluster counts depend on assumptions about the relationship between SZ flux and cluster mass (e.g., [38]). This is usually expressed as uncertainty in the hydrostatic mass bias parameter b where $M_X = (1-b)M_{500}$, M_X is a mass proxy derived from observed SZ flux with an assumption of hydrostatic equilibrium, and M_{500} is the true cluster halo mass (see [37,38] for more details). The bias parameter b itself is not well known today; e.g., constraints derived from gravitational shear mass measurements Weighing the Giants (WtG) [42], from Canadian Cluster Comparison Project (CCCP) [43], and from CMB Lensing (Lens) [44,57] listed as follows show significant uncertainties:

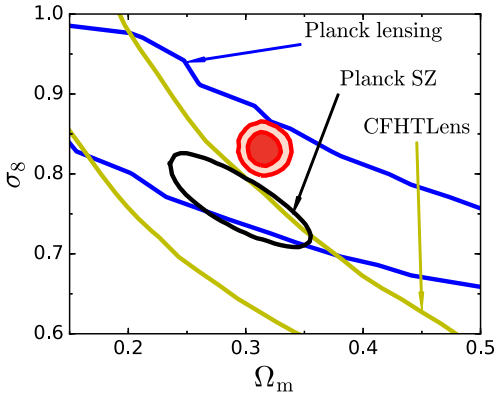

FIG. 3. The σ_8 tension in the ΛCDM cosmology, where the red filled contours (1σ and 2σ) are derived from Planck 2015 temperature and polarization, and the unfilled contours corresponding to the three LSS measurements are given at 2σ level, where the SZ contour is the constraint fixing the mass bias parameter as the baseline value $1-b=0.8$.

$$1-b = 0.688 \pm 0.072 \quad \text{[WtG]}, \tag{7a}$$

$$1-b = 0.780 \pm 0.092 \quad \text{[CCCP]}, \tag{7b}$$

$$1-b = 0.74 \pm 0.07 \quad \text{[Lens]}. \tag{7c}$$

As shown in [38], the σ_8 constraint derived from SZ cluster counts is sensitive to the prior used: the WtG prior almost eliminates the σ_8 tension between SZ and Planck CMB, while the CCCP prior remains in noticeable tension. In addition, a reference model fixing the bias parameter as the baseline value, $1-b=0.8$, was also investigated in the Planck SZ analysis [37], which yields the σ_8 constraint of Eq. (6c), in tension with that derived from Planck CMB at $\gtrsim 3\sigma$ confidence level (see also Fig. 3).

In previous analyses, the σ_8 constraint of Eq. (6c) was usually used as an approximation to the full Planck SZ data. It is natural to ask whether it is valid to fix the bias parameter as the baseline value in constraining the dm-drf interaction model, considering the large uncertainty in the bias parameter, the sensitive dependence of the σ_8 constraint on the bias parameter and the mild tension between the WtG constraint and the baseline value (see [58] for a summary of recent bias parameter inferences). We discuss this next.

B. Anaysis with SZ data: the impact of the mass bias parameter

To highlight the impact of the uncertainty in the SZ cluster counts on the model parameter constraints, we use both CMB and SZ data with the mass bias parameter fixed or varying, and compare the resulting constraints. For CMB data, we use Planck 2015 CMB temperature and polarization data TTTEEE + lowTEB [59] (PlanckTP). For SZ data with varying mass bias parameter, we use Planck 2015 SZ cluster counts data (PlanckSZ) with the CCCP prior, while for SZ data with fixed mass bias parameter, we use the single data point of Eq. (6c), as done in previous analyses.

We use CosmoMC to run MCMC chains, with flat priors on $N_{drf} \geq 0.07$ and $\Gamma_0 \geq 0$, and CosmoMC default priors for ΛCDM parameters and other nuisance parameters, where $N_{drf} = 0.07$ and $\Gamma_0 = 0$ are the physical lower limits of these parameters in the dm-drf interaction model

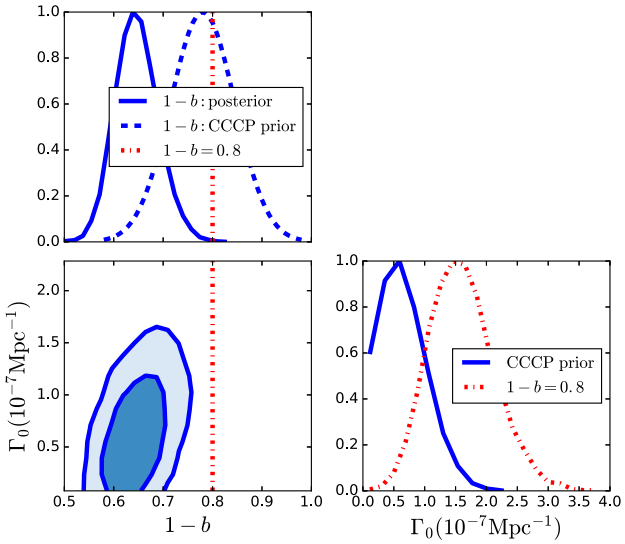

FIG. 4. The results of the two MCMC runs (red vs blue) for the canonical dm-drf model using joint data set PlanckTP+ PlanckSZ. Upper left panel: the comparison of the CCCP prior (blue/dashed) and the resulting posterior (blue/solid) with the baseline value $1-b=0.8$ (red/dot-dashed). Lower left panel: the posterior contour of $1-b$ vs Γ_0. Lower right panel: the marginalized posteriors of Γ_0 with the bias parameter fixed (red/dot-dashed) or varying (blue/solid).

we are considering [20,21]. The data disfavor large values for these two parameters, $N_{\rm drf} \gg 1$ and $\Gamma_0 \gg 10^{-7}$ Mpc^{-1}, so there is no need to truncate the prior ranges for these parameters. Our adopted priors are consistent with those used previously [21]. We use the Raferty and Lewis statistic $R-1 \leq 0.02$ as the convergence criterion, and we summarize the MCMC results in Fig. 4 and Table II.

We perform two different MCMC runs jointly using PlanckTP and PlanckSZ. In the first run, we fix the bias parameter as $1-b=0.8$ and obtain an inference of nonzero Γ_0 at 3σ significance (red/dot-dashed lines in Fig. 4), which is similar to previous works. In the second run, we let the bias parameter vary and impose the CCCP prior (blue/dashed line in Fig. 4). As a result, we only find an upper limit of Γ_0 (blue/solid lines in Fig. 4).

Why has the detection gone away? First, it is important to point out that the CMB likelihood alone disfavors large Γ_0 (see Table II). In the previous analyses, the combination of PlanckSZ and PlanckTP forced a solution away from what is preferred by the CMB likelihood alone. However, our introduction of some freedom in the bias parameter allows the other parameters to adjust, as preferred by the CMB data, since the low number counts of PlanckSZ can now be explained by a downward shift in $1-b$ rather than a low σ_8. The CMB preference for $10^7\Gamma_0/\mathrm{Mpc}^{-1} < 1.28$ at 95% confidence is the reason the contour in Fig. 4 closes at the upper end, constraining $1-b$ to lower values. The posterior of the mass bias parameter turns out to converge at $1-b=0.647\pm0.044$, which is about 1.5σ lower than the baseline value 0.8 and 2 times tighter than the CCCP prior imposed, where σ here is the σ of the prior constraint on $1-b$.

We also checked the approximation of using the single data point of Eq. (6c) rather than the full SZ likelihood. Equation (6c) follows from the full SZ likelihood given the ΛCDM model and that $1-b=0.8$ with no uncertainty. We find the approximation works well. We find very similar constraints on the dm-drf interaction model parameters whether we use the full SZ likelihood (and $1-b=0.8$) or approximate it with Eq. (6c). Both of them result in an inference of nonzero dm-drf interaction at $\sim 3\sigma$ significance, with tiny differences in the mean values and the uncertainties, which do not affect our conclusion. We therefore do not distinguish the two cases in this paper.

From Table II, we also see that PlanckSZ with the CCCP prior is not highly constraining; adding it to PlanckTP only slightly increases the upper limits of Γ_0 and $N_{\rm drf}$. It is clear that the other two priors would lead to even less of a nonzero Γ_0 preference, which can be verified by the fact that the tension of the $1-b$ posterior with the CCCP prior is greater than its tension with the WtG/Lens prior.

C. Analysis with only CMB Lensing and DES data

Since the SZ data (with the bias parameter allowed to float) is not highly constraining, we drop it from further consideration as we examine the dm-drf model with PlanckTP and the following two LSS data sets:

(1) Lensing: Planck 2015 lensing data [30].
(2) DES: $\sigma_8(\Omega_{\rm m}/0.3)^{0.5}=0.789\pm0.026$, which is derived from the DES first-year cosmic shear data [35] and is a slightly tighter constraint than that derived from CFHTLens [Eq. (6b)] or from KiDS-450 [32].

TABLE II. Constraints on the dm-drf model parameters using data sets PlanckTP, PlanckSZ, Lensing and DES, where the uncertainties are 1σ values, and the upper limits are given at 2σ confidence level.

		PlanckTP + PlanckSZ		
Data set	PlanckTP	$1-b=0.78\pm0.092$	$1-b=0.8$	PlanckTP + Lensing + DES
$1-b$		0.647 ± 0.044		
$\Gamma_0(10^{-7}$ Mpc$^{-1})$	<1.28	<1.36	1.61 ± 0.54	<1.43
$N_{\rm drf}$	<0.57	<0.62	<0.64	<0.67
σ_8	0.817 ± 0.022	0.807 ± 0.019	0.758 ± 0.015	0.800 ± 0.016

Strictly speaking, we should use the DES likelihood with all the relevant nuisance parameters (e.g., the intrinsic alignment of galaxies) varying, instead of using this single data point. But the likelihood code is not publicly available, and as we see later, we find no detection of the dm-drf interaction. Therefore we expect no qualitative difference using the single data point versus using a full likelihood with proper treatment of uncertainties.

The MCMC results are summarized in Table II. Again, we find no detection of the dm-drf interaction using the joint data set PlanckTP + Lensing + DES, though it is more constraining than another joint data set PlanckTP + PlanckSZ with the CCCP prior.

IV. Lyman-α FOREST DATA

Lyα forest observations have been used as a cosmological probe for the past two decades (e.g., [60–62]). Lyα absorption is sensitive to the density of neutral gas in a relatively low-density, smooth environment, which is tightly correlated with the underlying dark matter density on large scales. Many of these observational results are based on a direct measurement of the Lyα forest power spectrum $P_F(k)$, a statistical property of the transmitted flux fluctuations

$$\delta_F(\lambda) = e^{-\tau(\lambda)}/\langle e^{-\tau(\lambda)}\rangle - 1, \tag{8}$$

where λ is the observed wavelength of Lyα emission, and τ is the optical depth to Lyα absorption. The tight correlation between the neutral gas density and the underlying dark matter density allows a determination of the matter power spectrum from the Lyα forest power spectrum $P_F(k)$. For this purpose, hydrodynamical simulations are required to compute $P_F(k)$ for a given initial linear matter power spectrum $P_L(k, z_i)$ at some high redshift z_i, due to the complexities in the nonlinear evolution of dark matter and hydrodynamical processes.

Compared with CMB data and LSS measurements including DES and Planck SZ, the latest measurements [46–48] of the Lyα forest flux power spectrum from the Baryon Oscillation Spectroscopic Survey extend sensitivity to the matter power spectrum to smaller scales. The constraints on the amplitude $\Delta_L^2 = k^3 P_L(k, z)/2\pi^2$ and the slope $n_{\rm eff} = d\ln P_L(k, z)/d\ln k$ at $k = 0.009$ (s/km) $\times$ $H(z)/(1+z)$ and $z = 3$ are explicitly given in [47], where $H(z)$ is the Hubble expansion rate.

These two parameters (Δ_L^2 and $n_{\rm eff}$) were introduced to capture the constraints of the Lyα forest measurements on the power spectrum in ΛCDM-like models [45]. These include models with primordial power spectra where the tilt changes with k in a smooth manner. If the changes introduced in the linear power spectrum by the dm-drf models are similar and small ($\mathcal{O}(10\%)$), as is the case for the preferred models, these variables may be used to impose constraints from Lyα forest flux measurements.

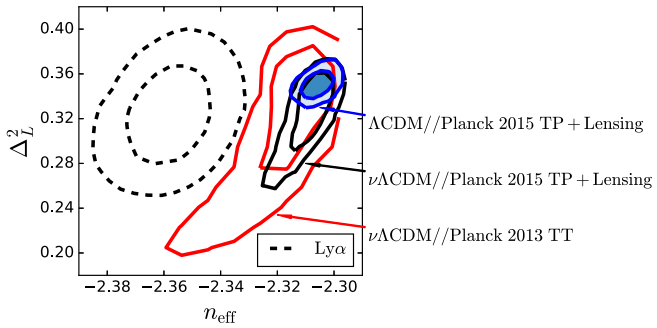

FIG. 5. The tension between Lyα and CMB in ΛCDM cosmology with neutrino mass fixed as 0.06 eV (ΛCDM) or varying ($\nu\Lambda$CDM) where Δ_L^2 and $n_{\rm eff}$ are the amplitude and the slope of the linear matter power spectra at $k \simeq h\,{\rm Mpc}^{-1}$ and at $z = 3$.

As pointed out in [63], the matter power spectrum derived from the Lyα forest data yields a comparable amplitude but a much steeper slope at scale $k \sim {\rm Mpc}^{-1}$, compared with those derived from Planck CMB data, assuming ΛCDM. We plot these constraints in Fig. 5, which clearly shows that inferences of the matter power spectrum from the Lyα forest data are highly inconsistent with the Planck CMB data, assuming ΛCDM. The discrepancy has increased from the first release of Planck data to the second, since the second yields a flatter slope $n_{\rm eff}$ with a reduced uncertainty (likely due to a larger $n_{\rm s}$ and a tighter constraint on $\omega_{\rm m}$ [59]). Allowing neutrino mass to vary does not do much to reconcile the discrepancy in the matter power slope $n_{\rm eff}$.

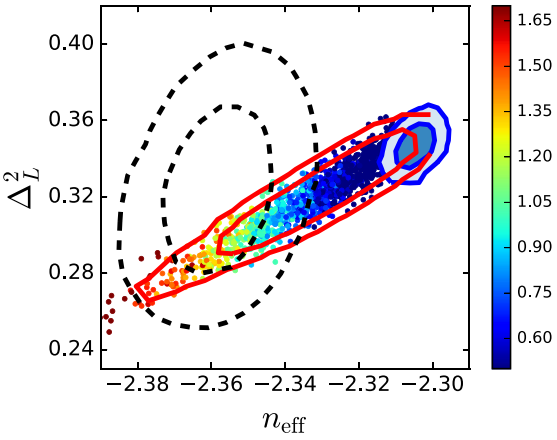

FIG. 6. Comparison of the Lyα constraints on the amplitude Δ_L^2 and the slope $n_{\rm eff}$ of the matter power spectrum with those derived from ΛCDM (blue filled contours) and the dm-drf interaction model (red unfilled contours) using PlanckTP + Lensing + DES, where the color points denote different Γ_0 values in unit of 10^{-7} Mpc^{-1}.

The steeper slope $n_{\rm eff}$ derived from Lyα data at scale $k \sim$ Mpc^{-1} implies a scale-dependent matter power suppression which aligns well with the dm-drf interaction picture. To examine whether the Lyα data are in agreement with other data sets in the dm-drf interaction model, we plot the $\Delta_L^2 - n_{\rm eff}$ contours derived from PlanckTP+Lensing+DES in Fig. 6. We see that the joint data set favors the dm-drf interaction model (with interaction rate $10^7\Gamma_0/\mathrm{Mpc}^{-1}$ in the range of [0.9, 1.6]).

Our results serve to highlight the potential importance of these inferences of the matter power spectrum from the Lyα data. If they are substantially free from bias and have adequately captured all significant sources of uncertainty, then the discrepancy with the Planck-conditioned predictions of ΛCDM is extremely interesting. Possible solutions to this discrepancy include the dark matter model we are studying here, as well as a negative running $dn_s/d\ln k$ [48,63] or possibly a different dm-drf interaction.

V. GENERALIZED DM-DRF MODELS

We have been focused on exploring the possibility of resolving the σ_8 tension and the Lyα-CMB tension via the non-Abelian dark sector model, which is featured with a dark matter scattering rate $\Gamma \propto T^2$. In this model, the dm-drf interaction gives rise to a smooth and featureless suppression in the matter power spectrum due to a constant scattering rate over expansion rate ratio Γ/H in the radiation-dominated era. As shown in some recent works (e.g., [24,25]), there is in fact a large class of interacting dm-drf models distinguished by different scalings $\Gamma = \Gamma_0(T/T_0)^\beta$, with scaling index β varying from 0 to 6. For all these dm-drf models with scaling index different from 2, we also expect a net suppression in the matter power spectrum and therefore a smaller σ_8, though the matter power spectrum suppression would be characterized by a new length scale which enters the horizon when Γ approaches H.

To explore the implications of $\beta \neq 2$ for relevant observables, we examine the $\beta = 1$ and $\beta = 3$ cases in this section. We first briefly discuss the imprints of the generalized dm-drf interaction rates on the CMB power spectra and the matter power spectrum, then constrain these models using CMB data and LSS measurements.

The imprints of the three different models on the matter power spectrum suppression are pretty distinct at small scales, as shown in Fig. 7. For $\beta = 3$, dark matter and dark radiation are tightly coupled deep in the radiation-dominated era. Dark matter perturbations oscillate instead of growing; therefore all modes entering the horizon when $\Gamma \gtrsim H$ are strongly suppressed. In the $\beta = 1$ case, the interaction is negligible at early time. For sufficiently small modes entering horizon early, the power suppression is dominated by late time when the dm-drf interaction becomes important. For large modes entering horizon when $\rho_{\rm drf}/\rho_{\rm dm}$ becomes vanishingly small, the dark matter overdensity growth is unaffected by the interaction. For the intermittent modes, the power suppression is determined by several factors, including the coupling strength today Γ_0, the matter-radiation equality where the Γ/H dependence on the scale factor changes, and the dark matter and dark radiation energy density ratio $\rho_{\rm drf}/\rho_{\rm dm}$. Therefore we see a power suppression plateau on the small-scale end, no suppression on the large-scale end, and a smooth transition in between. Different from the $\beta = 2$ case, both $\beta = 1$ and $\beta = 3$ interactions introduce new length scales to the matter power suppression.

Following the argument given in Sec. II B, it is not hard to figure out the impacts of the general interaction rates on the temperature and polarization power spectra. For example, we expect that the $\beta = 3$ interaction tends to suppress

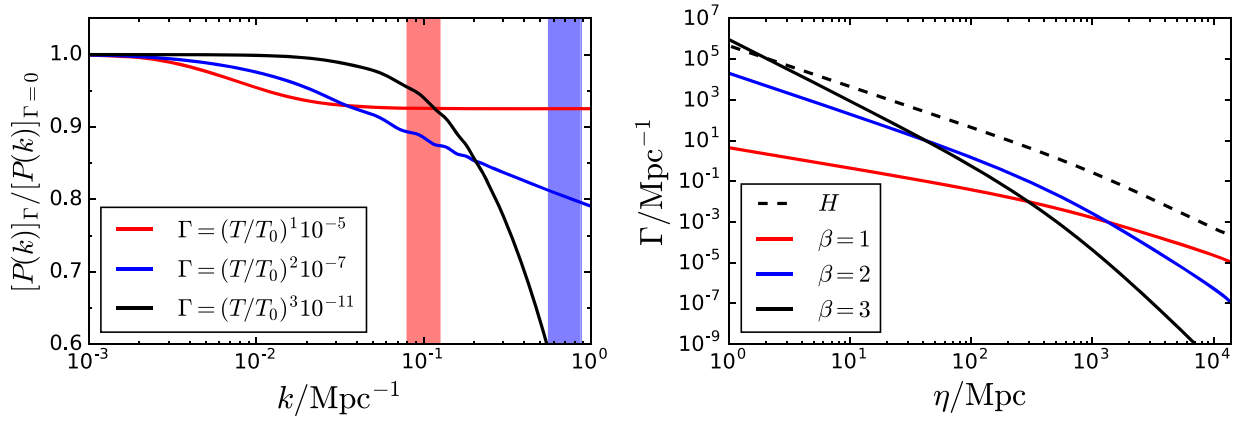

FIG. 7. Left panel: The matter power spectrum suppression from different dm-drf interaction rates $\Gamma = \Gamma_0(T/T_0)^\beta$ (with $\Gamma_0/\mathrm{Mpc}^{-1} = 10^{-5}$, 10^{-7}, 10^{-11} for $\beta = 1$, 2, 3, respectively), where the red band denotes the modes σ_8 is sensitive to and the blue band denotes the modes Lyα measurement is sensitive to. Right panel: the comparison between the Hubble expansion rate and the dm-drf interaction rates.

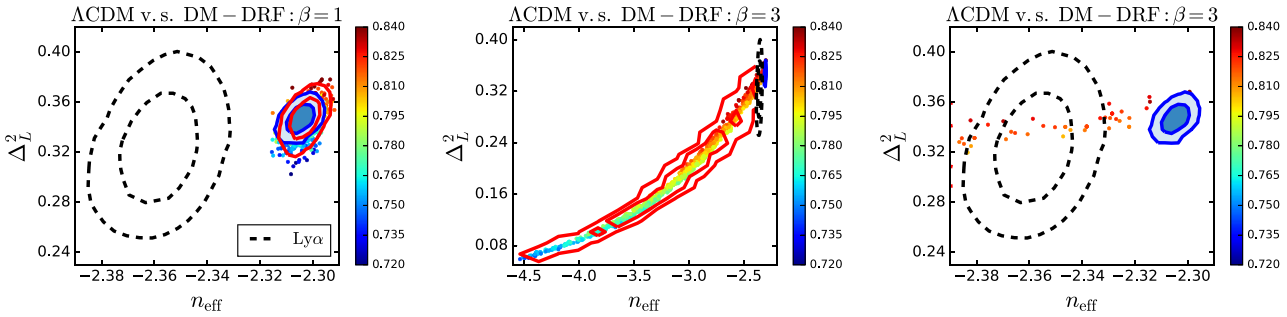

FIG. 8. Comparison of the Lyα constraint on the amplitude Δ_L^2 and the slope $n_{\rm eff}$ of the matter power spectrum with those derived from ΛCDM and dm-drf interaction models using PlanckTP + Lensing + DES, where the blue filled contours are the results of the ΛCDM cosmology, the red unfilled contours are the results of the dm-drf models, and the color bars denote σ_8 for dm-drf with $\beta = 1$, 3, respectively. Two right panels show the same $\beta = 3$ model but with different ranges on the x axis.

the amplitudes of large k modes entering the horizon at radiation domination and when Γ/H is noticeable, while leaving no imprint on the amplitudes of small k modes entering the horizon when Γ/H is negligible; on the contrary, the $\beta = 1$ interaction should only affect large k modes. We have modified CAMB to allow for all three interaction models, and numerical results confirm our qualitative expectations above. We find that the imprints of the three different models are too subtle to be distinguished via Planck CMB data, so we do not plot them here.

We constrain the two models using the joint data set PlanckTP + Lensing + DES, finding no detection of interaction for either of the two new cases. Similar to the previous section, we also examine whether these two models reconcile the Lyα-CMB tension. As shown in Fig. 8, the $\beta = 1$ interaction does not change the amplitude and the slope much, and the $\beta = 3$ interaction leads to an overwhelming suppression. We see that neither of the two help to reconcile the Lyα-CMB tension.

VI. SUMMARY

In this paper, we reinvestigated the non-Abelian dark sector model proposed by [20]. We examined the impact of the dm-drf interaction on the CMB power spectra and the matter power spectrum in detail. We found that the dm-drf interaction affects the amplitudes of CMB power spectra by modifying the gravitational potential decay, but only slightly. We verified the presence of a logarithmic suppression in the matter power spectrum that originates from the self-similar suppression of the matter overdensity. We also constrained the dm-drf model using CMB and LSS measurements in a more systematic way.

We found that Planck SZ plays the key role in the previously claimed inference of nonzero dm-drf interaction. However the SZ cluster counts constraint is limited by uncertainty in the cluster mass scale determination, which is usually parametrized as the mass bias parameter b. We confirmed the inference of nonzero dm-drf interaction at 3σ significance using the Planck data and the SZ data fixing the bias parameter to be constant, $1 - b = 0.8$, as done in previous analyses. But, when we included uncertainties in $1 - b$, the preference of nonzero dm-drf interaction essentially disappeared.

We also show that the latest inferences of the matter power spectrum from Lyα forest data are highly inconsistent with the Planck CMB data, assuming ΛCDM, and that the joint data sets favor a nonzero dark sector interaction. Thus if these matter power spectrum inferences are free from significant systematic error, and if the reported uncertainties accurately include all sources of uncertainty, these data are more sensitive to the impact of dm-drf interactions and provide us with a significant detection. Even so, there are other possible ways to reconcile the Planck and Lyα forest data such as a nonzero running of the scalar spectral index $dn_{\rm s}/d\ln k$ [48,63].

We also explored two different phenomenological dm-drf interaction models characterized by interaction rates scaling with temperature in different power laws, and found that neither of these interactions is favored by current CMB and LSS data.

We are unsure what to make of these inferences of the matter power spectrum from the Lyα forest data. We hope our work serves to motivate further study of these data. Were a different group to reach similar conclusions independently, even if from the same data, that would bolster our confidence. Another avenue for progress is measurements that can decrease uncertainty in $1 - b$ as the cluster mass function has the statistical power to make a detection absent that uncertainty, if the interaction strength is at the higher end of the range consistent with Lyα data.

ACKNOWLEDGMENTS

We thank Julien Lesgourgues for helpful comments on an earlier version of the manuscript. Z. P. thanks Lachlan Lancaster for his valuable help in modifying CAMB.

Z. P. is supported by the UC Davis Dissertation Year Fellowship. M. K. is supported by the National Science Foundation Grant No. PHY-1620638. This work made extensive use of the NASA Astrophysics Data System and of the astro-ph preprint archive at arXiv.org. All the computations and plots are done with the Boltzmann codes CAMB and CLASS, and MCMC codes Cosmomc, MontePython and Cosmoslik.

[1] R. H. Sanders, *The Dark Matter Problem: A Historical Perspective* (Cambridge University Press, Cambridge, 2010).
[2] G. Bertone and D. Hooper, arXiv:1605.04909.
[3] J. G. De Swart, G. Bertone, and J. Van Dongen, Nat. Astron. **1**, 0059 (2017).
[4] E. Aprile *et al.* (XENON), Phys. Rev. Lett. **119**, 181301 (2017).
[5] J. V. Sloan *et al.*, Phys. Dark Universe **14**, 95 (2016).
[6] J. March-Russell, S. M. West, D. Cumberbatch, and D. Hooper, J. High Energy Phys. 07 (2008) 058.
[7] J. L. Feng and J. Kumar, Phys. Rev. Lett. **101**, 231301 (2008).
[8] J. L. Feng, H. Tu, and H.-B. Yu, J. Cosmol. Astropart. Phys. 10 (2008) 043.
[9] C. Cheung, G. Elor, L. J. Hall, and P. Kumar, J. High Energy Phys. 03 (2011) 042.
[10] J. L. Feng, M. Kaplinghat, H. Tu, and H.-B. Yu, J. Cosmol. Astropart. Phys. 07 (2009) 004.
[11] F.-Y. Cyr-Racine and K. Sigurdson, Phys. Rev. D **87**, 103515 (2013).
[12] CMB-S4 Collaboration, arXiv:1610.02743.
[13] D. E. Kaplan, G. Z. Krnjaic, K. R. Rehermann, and C. M. Wells, J. Cosmol. Astropart. Phys. 05 (2010) 021.
[14] D. E. Kaplan, G. Z. Krnjaic, K. R. Rehermann, and C. M. Wells, J. Cosmol. Astropart. Phys. 10 (2011) 011.
[15] R. Diamanti, E. Giusarma, O. Mena, M. Archidiacono, and A. Melchiorri, Phys. Rev. D **87**, 063509 (2013).
[16] M. Archidiacono, S. Hannestad, R. S. Hansen, and T. Tram, Phys. Rev. D **91**, 065021 (2015).
[17] Z. Chacko, Y. Cui, S. Hong, T. Okui, and Y. Tsai, J. High Energy Phys. 12 (2016) 108.
[18] F. Y. Cyr-Racine, K. Sigurdson, J. Zavala, T. Bringmann, M. Vogelsberger, and C. Pfrommer, Phys. Rev. D **93**, 123527 (2016).
[19] V. Prilepina and Y. Tsai, J. High Energy Phys. 9 (2017) 33.
[20] M. A. Buen-Abad, G. Marques-Tavares, and M. Schmaltz, Phys. Rev. D **92**, 023531 (2015).
[21] J. Lesgourgues, G. Marques-Tavares, and M. Schmaltz, J. Cosmol. Astropart. Phys. 02 (**2016**) 037.
[22] P. Ko and Y. Tang, Phys. Lett. B **768**, 12 (2017).
[23] P. Ko, N. Nagata, and Y. Tang, Phys. Lett. B **773**, 513 (2017).
[24] Y. Tang, Phys. Lett. B **757**, 387 (2016).
[25] Y. Tang, Mod. Phys. Lett. A **32**, 1740006 (2017).
[26] R. Krall, F.-Y. Cyr-Racine, and C. Dvorkin, J. Cosmol. Astropart. Phys. 09 (2017) 003.
[27] M. Raveri, W. Hu, T. Hoffman, and L.-T. Wang, Phys. Rev. D **96**, 103501 (2017).
[28] M. A. Buen-Abad, M. Schmaltz, J. Lesgourgues, and T. Brinckmann, J. Cosmol. Astropart. Phys. 01 (2018) 008.
[29] E. Di Valentino, C. B. Hm, E. Hivon, and F. R. Bouchet, Phys. Rev. D **97**, 043513 (2018).
[30] Planck Collaboration XV, Astron. Astrophys. **594**, A15 (2016).
[31] C. Heymans *et al.*, Mon. Not. R. Astron. Soc. **432**, 2433 (2013).
[32] H. Hildebrandt *et al.*, Mon. Not. R. Astron. Soc. **465**, 1454 (2017).
[33] F. Köhlinger, M. Viola, B. Joachimi, H. Hoekstra, E. van Uitert, H. Hildebrandt, A. Choi, T. Erben, C. Heymans, S. Joudaki, D. Klaes, K. Kuijken, J. Merten, L. Miller, P. Schneider, and E. A. Valentijn, Mon. Not. R. Astron. Soc. **471**, 4412 (2017).
[34] DES Collaboration, arXiv:1708.01530.
[35] DES Collaboration, arXiv:1708.01538.
[36] B. A. Benson *et al.*, Astrophys. J. **763**, 147 (2013).
[37] Planck Collaboration XX, Astron. Astrophys. **571**, A20 (2014).
[38] Planck Collaboration XXIV, Astron. Astrophys. **594**, A24 (2015).
[39] A. G. Riess, L. M. Macri, S. L. Hoffmann, D. Scolnic, S. Casertano, A. V. Filippenko, B. E. Tucker, M. J. Reid, D. O. Jones, J. M. Silverman, R. Chornock, P. Challis, W. Yuan, P. J. Brown, and R. J. Foley, Astrophys. J. **826**, 56 (2016).
[40] B. Follin and L. Knox, arXiv:1707.01175.
[41] S. Das, R. Mondal, V. Rentala, and S. Suresh, arXiv: 1712.03976.
[42] A. Von der linden, M. T. Allen, D. E. Applegate, P. L. Kelly, S. W. Allen, H. Ebeling, P. R. Burchat, D. L. Burke, D. Donovan, R. G. Morris, R. Blandford, T. Erben, and A. Mantz, Mon. Not. R. Astron. Soc. **439**, 2 (2014).
[43] H. Hoekstra, R. Herbonnet, A. Muzzin, A. Babul, A. Mahdavi, M. Viola, and M. Cacciato, Mon. Not. R. Astron. Soc. **449**, 685 (2015).
[44] J.-B. Melin and J. G. Bartlett, Astron. Astrophys. **578**, A21 (2015).
[45] P. McDonald *et al.* (SDSS), Astrophys. J. **635**, 761 (2005).
[46] N. Palanque-Delabrouille *et al.*, Astron. Astrophys. **559**, A85 (2013).
[47] N. Palanque-Delabrouille, C. Yèche, J. Lesgourgues, G. Rossi, A. Borde, M. Viel, E. Aubourg, D. Kirkby, J.-M. LeGoff, J. Rich, N. Roe, N. P. Ross, D. P. Schneider, and D. Weinberg, J. Cosmol. Astropart. Phys. 02 (2015) 045.
[48] N. Palanque-Delabrouille, C. Yeche, J. Baur, C. Magneville, G. Rossi, J. Lesgourgues, A. Borde, E. Burtin, J.-M. LeGoff, J. Rich, M. Viel, and D. Weinberg, J. Cosmol. Astropart. Phys. 11 (2015) 011.

[49] B. Follin, L. Knox, M. Millea, and Z. Pan, Phys. Rev. Lett. **115**, 091301 (2015).
[50] W. Hu and N. Sugiyama, Astrophys. J. **471**, 542 (1996).
[51] W. Hu and M. White, Astrophys. J. **471**, 30 (1996).
[52] W. Hu and M. White, Astrophys. J. **479**, 568 (1997).
[53] S. Bashinsky and U. Seljak, Phys. Rev. D **69**, 083002 (2004).
[54] S. Bashinsky, arXiv:0707.0692.
[55] D. Baumann, D. Green, J. Meyers, and B. Wallisch, J. Cosmol. Astropart. Phys. 01 (**2016**) 007.
[56] Z. Pan, L. Knox, B. Mulroe, and A. Narimani, Mon. Not. R. Astron. Soc. **459**, 2513 (2016).
[57] G. Hurier and R. E. Angulo, Astron. Astrophys. **610**, L4 (2018).
[58] L. Salvati, M. Douspis, and N. Aghanim, arXiv:1708.00697.
[59] Planck Collaboration XIII, Astron. Astrophys. **594**, A13 (2016).
[60] R. A. C. Croft, D. H. Weinberg, N. Katz, and L. Hernquist, Astrophys. J. **495**, 44 (1998).
[61] P. McDonald, J. MiraldaEscude, M. Rauch, W. L. W. Sargent, T. A. Barlow, R. Cen, and J. P. Ostriker, Astrophys. J. **543**, 1 (2000).
[62] P. McDonald, U. Seljak, S. Burles, D. J. Schlegel, D. H. Weinberg, R. Cen, D. Shih, J. Schaye, D. P. Schneider, N. A. Bahcall, J. W. Briggs, J. Brinkmann, R. J. Brunner, M. Fukugita, J. E. Gunn, Ž. Ivezić, S. Kent, R. H. Lupton, and D. E. Vanden Berk, Astrophys. J. Suppl. Ser. **163**, 80 (2006).
[63] Q. E. Minor and M. Kaplinghat, Phys. Rev. D **91**, 063504 (2015).